

**Electronic supplementary information**

**Highly Sensitive Mutation Quantification by High-Dynamic-Range Capillary-Array  
Electrophoresis (HiDy CE)**

Takashi Anazawa<sup>\*a</sup>, Hiroko Matsunaga<sup>ac</sup>, Shuhei Yamamoto<sup>b</sup>, and Ryoji Inaba<sup>b</sup>

<sup>a</sup>Research and Development Group, Hitachi, Ltd., 1-280 Higashi-koigakubo, Kokubunji,  
Tokyo 185-8601, Japan

<sup>b</sup>Science & Medical Systems Business Group, Hitachi High-Technologies Corporation,  
882 Ichige, Hitachinaka, Ibaraki 312-8504, Japan

<sup>c</sup>Present address: Research Organization for Nano and Life Innovation, Waseda  
University, 513 Waseda-tsurumaki-cho, Shinjuku, Tokyo 162-0041, Japan

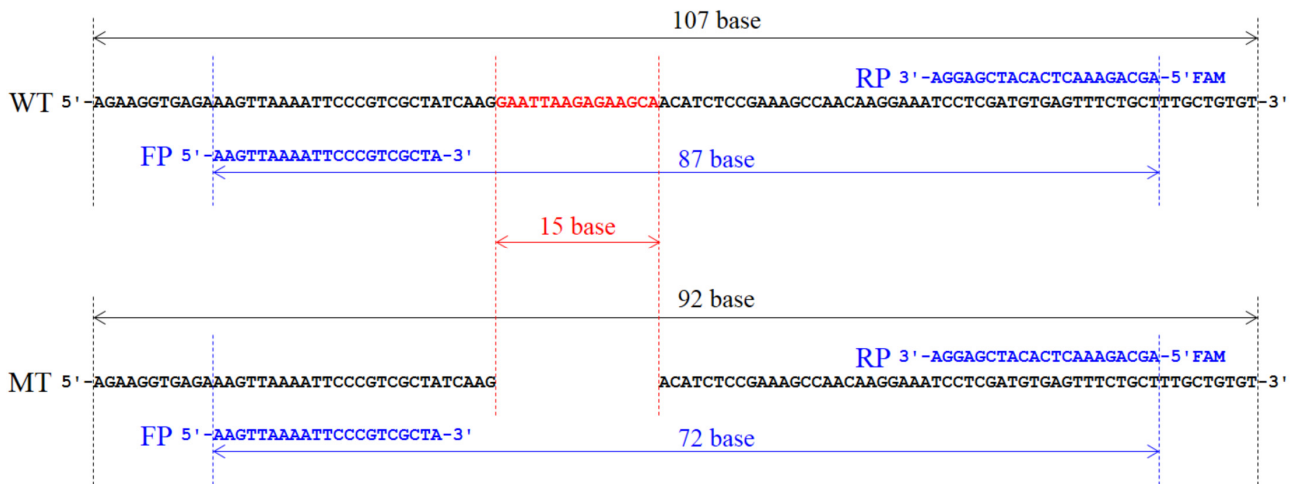


Fig. S-1

Assay design for quantification of MT (EGFR exon 19 with 15-base deletion) in a large excess of WT (EGFR exon 19). Sequences of WT, MT, a forward primer (FP), and a FAM-labeled reverse primer (RP) are shown. Base lengths of competitive-PCR products of WT and MT are also shown (87 and 72 bases, respectively).

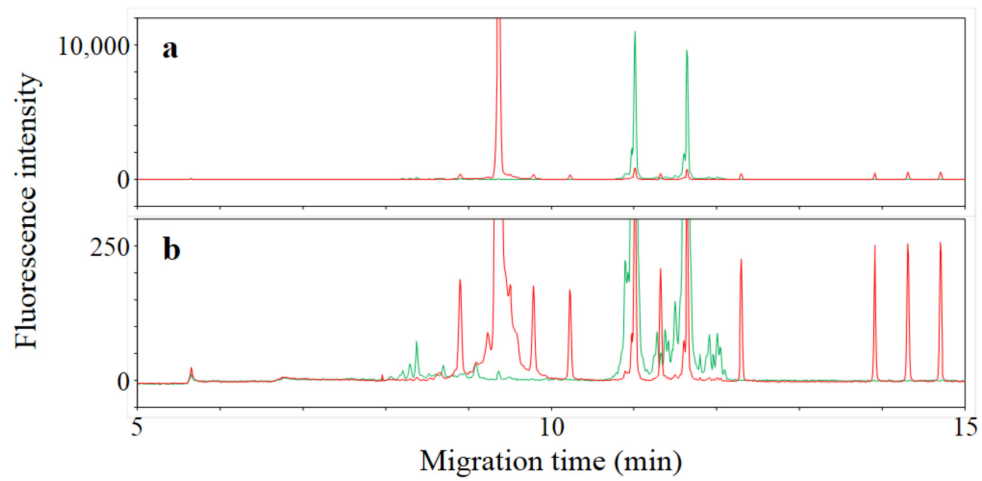


Fig. S-2

Typical raw electropherograms for a sample of 100% MT/WT separated in a capillary. Time courses of green and red fluorescence intensities are indicated by green and red lines, respectively. Green and red fluorescence intensities were derived from fluorescence intensities of green and red images shown in Fig. 3a, respectively. The same data is used but only vertical scales are changed in **a** and **b**.

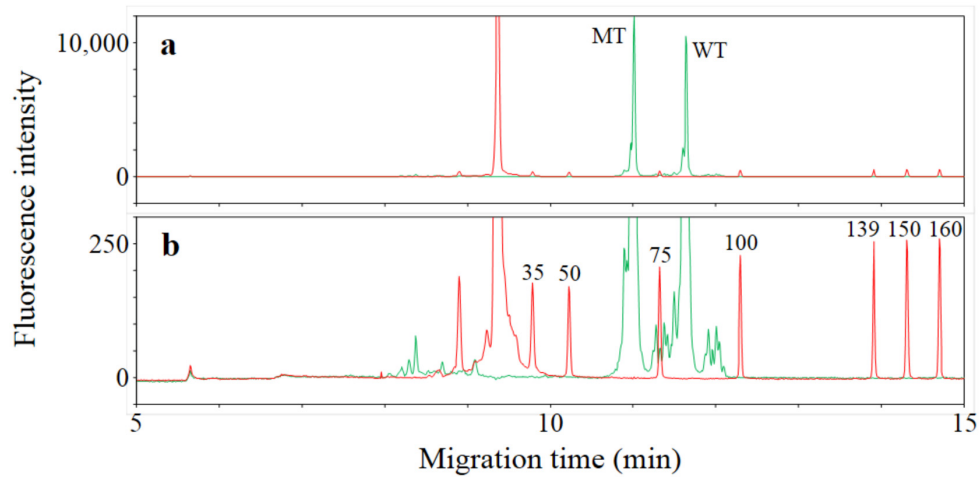


Fig. S-3

FAM and ROX electropherograms derived from the raw electropherograms in Fig. S-2. Time courses of FAM and ROX fluorescence intensities are indicated by green and red lines, respectively. FAM and ROX intensities were obtained by deconvolution of green and red fluorescence intensities to remove spectral overlap between FAM and ROX fluorescence. The same data is used but only vertical scales are changed in **a** and **b**. FAM peaks of WT and MT and ROX peaks of 35, 50, 75, 100, 139, 150, and 160 base fragments (internal size standard) are denoted.

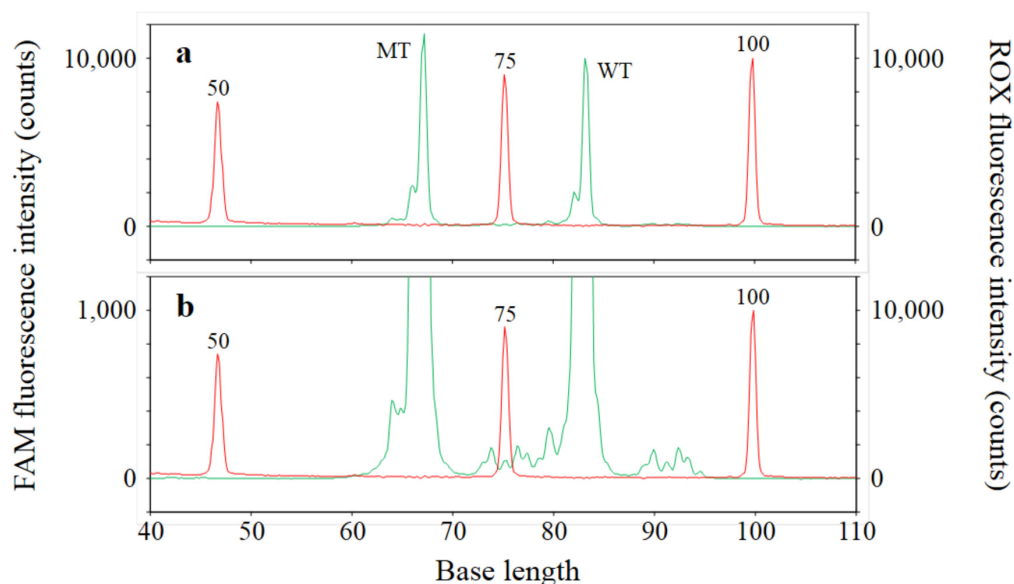


Fig. S-4

Normalized FAM and ROX electropherograms derived from the FAM and ROX electropherograms in Fig. S-3. Horizontal axis was converted from migration time to base length by using ROX peaks in Fig. S-3. FAM and ROX fluorescence intensities were normalized so that FAM fluorescence intensity of WT and ROX fluorescence intensity of the 100-base fragment were 10,000 counts, respectively. Left-hand and right-hand vertical axes indicate FAM and ROX fluorescence intensities, respectively. The same data is used in **a** and **b**, but only the left-hand vertical scales are changed from 0-10,000 in **a** to 0-1,000 in **b**, which correspond to the upper and lower images in Fig. 3b, respectively. FAM peaks of WT and MT and ROX peaks of 50, 75, and 100 base fragments are denoted.

## Reproducibility of capillary-array mounting.

Attachment of a four-capillary array with a four-lens array as shown in Fig. 1e on an image sensor with a four-dichroic-mirror array as shown in Fig. 2, and detachment of the four-capillary array with the four-lens array from the image sensor with the four-dichroic-mirror array were alternately repeated nineteen times. The first attachment numbered A1 was performed first, then the first detachment numbered D1, the second attachment numbered A2, and so on until the nineteenth attachment numbered A19. That is, the n-th attachment and the n-th detachment are numbered An and Dn, respectively. Through all the above processes, 70% formamide aqueous solution containing 100 nM dR6G dye-labeled C primer (ABI Prism BigDye Primer Cycle Sequencing Ready Reaction Kit, Thermo Fisher Scientific) was continuously flowing in all the four capillaries. In each attachment state (A1 to A19), the laser beam irradiated the four detection points of the four capillaries as shown in Fig. 2, and fluorescence of dR6G was emitted from each detection point. A sensor image containing four-color fluorescence images of the four capillaries was then acquired as shown in Fig. 3a. On the other hand, in each detachment state (D1 to D18), because the laser beam was fixed through all the processes, the laser beam did not irradiate any of the four capillaries. Therefore a sensor image without fluorescence images was acquired instead.

As an example, Fig. S-5 shows the acquired sensor images at A1, D1, A2, D18, and A19. The sensor images at A1, A2, and A19 contain almost the same four-color fluorescence images of the four capillaries (total sixteen images). As in Fig. 3a, fluorescence images of capillaries 1, 2, 3, and 4 are arranged vertically from top to bottom, and green, yellow, orange, and red fluorescence images are arranged horizontally from left to right. The sensor images at A3 to A18 (not shown) also contain almost the same images, respectively. On the other hand, the sensor images at D1 and D18 do not show anything. The sensor images at D2 to D17 (not shown) also do not show anything, respectively. The above results indicate that the four-capillary array with the four-lens array can be mounted at the exact position on the image sensor with the four-dichroic-mirror array by the positioning pins and magnets (not shown) with high reproducibility.

Regions of interest (ROIs) were defined at positions of green, yellow, orange, and red fluorescence images of capillary 1 in the sensor images. Then, green, yellow, orange, and red fluorescence intensities of capillary 1 were obtained by averaging pixel intensities in the corresponding ROIs. Fig. S-6 shows green, yellow, orange, and red fluorescence intensities of capillary 1 at A1 to A19 and at D1 to D18. Green, yellow, orange, and red fluorescence intensities of capillary 1 from A1 to A19 are  $5112 \pm 61$ ,  $23969 \pm 171$ ,  $10906 \pm 63$ , and  $3629 \pm 20$  (average  $\pm$  standard deviation), corresponding CV of 1.2%, 0.7%, 0.6%, and 0.6%, respectively. On the contrary, green, yellow, orange, and red fluorescence intensities of capillary 1 from D1 to D18 are  $423 \pm 0.5$ ,  $423 \pm 0.4$ ,  $419 \pm 0.5$ , and  $416 \pm 0.4$ . These are approximately offset (dark) levels of the image

sensor. These are therefore proofs that the four-capillary array with the four-lens array are completely detached from the image sensor with the four-dichroic-mirror. The above results demonstrate the high reproducibility of the capillary-array mounting much more clearly than results in Fig. S-5.

The above also allows the following. When a four-capillary array and a four-lens array are assembled and mounted on an image sensor with a four-dichroic-mirror array in a manufacturing plant so that performances of four-color-fluorescence detection of the four capillaries meet the standard values, and when the four-capillary array with the four-lens array is mounted on another image sensor with a four-dichroic-mirror array owned by a user, equivalent performances can be obtained.

Fig. S-5 and Fig. S-6 correspond to Fig. 6b and yellow bars in Fig. 7a of reference 31, respectively. Slight differences in ratios of green, yellow, orange, and red fluorescence intensities in both cases is due to slight differences in both fluorescence detection systems including the four-lens arrays.

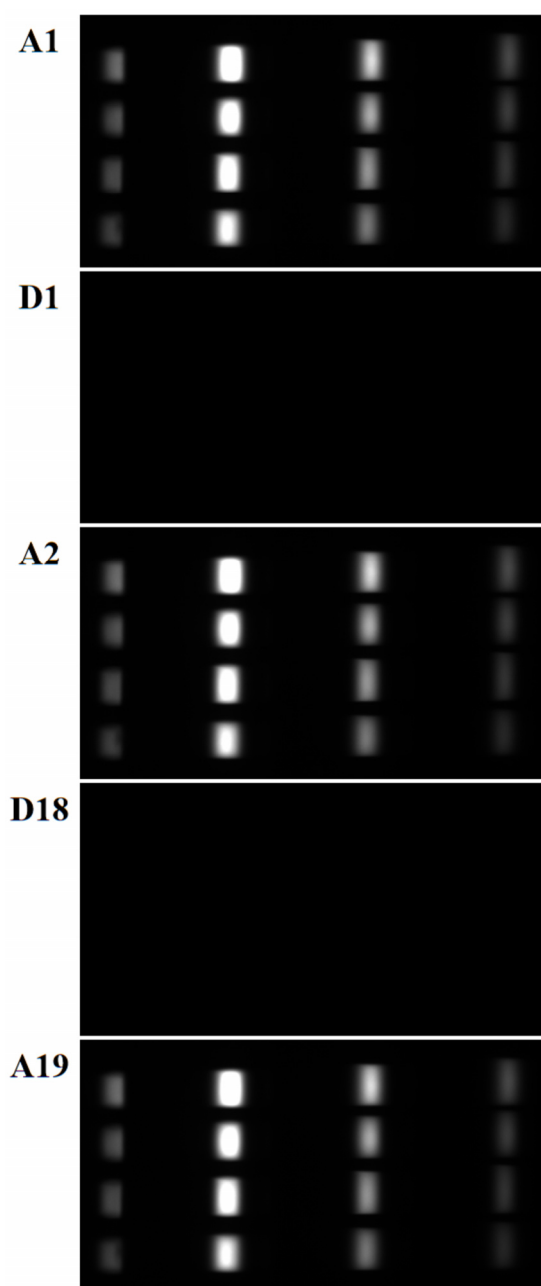


Fig. S-5

Sensor images when the four-capillary array with the four-lens array was repeatedly attached on and detached from the image sensor with the four-dichroic-mirror array. A1, A2, and A19 show sensor images at the 1st, 2nd, and 19th attachments, respectively. Four-color-fluorescence images of the four capillaries containing 100-nM dR6G are observed in each sensor image. D1 and D18 show sensor images at the 1st and 18th detachments, respectively. No fluorescence image is observed in each sensor

image. Gray scale of 400 – 30000 is common in all the sensor images.

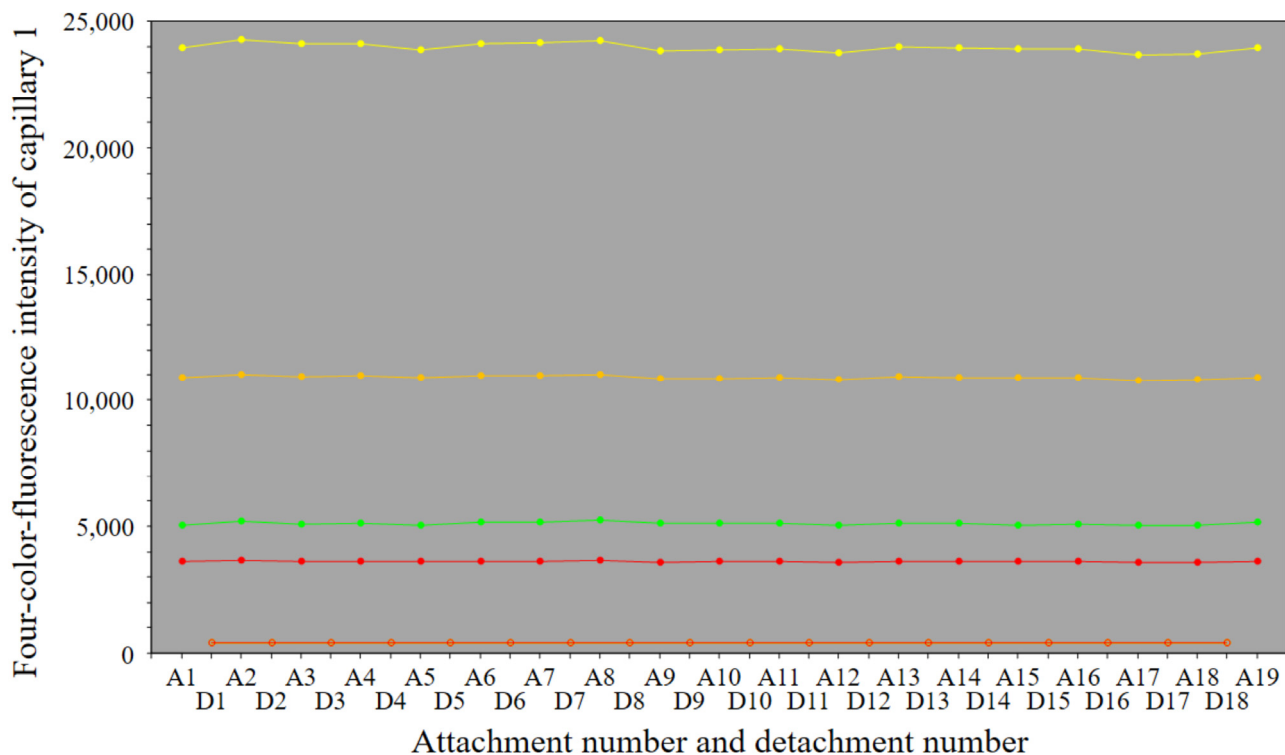


Fig. S-6

Four-color-fluorescence intensities of capillary 1 at A1 to A19 (closed circular plots) and D1 to D18 (open circular plots), where the n-th attachment and the n-th detachment are numbered An and Dn, respectively, in the same experiment as in Fig. S-5. Green, yellow, orange, and red plots and lines indicate green, yellow, orange, and red fluorescence intensities, respectively.